Supporting Information

Dardaei et al. 10.1073/pnas.1321200111

SI Materials and Methods

Antibodies. Pbx-regulating protein-1 (Prep1), pre–B-cell leukemia homeobox-1 (Pbx1), and Pbx2 antibodies were purchased from Santa Cruz Biotechnology. Myeloid ecotropic viral integration site-1 (Meis1) antibody was provided by Miguel Torres (Centro Nacional de Investigaciones Cardiovasculares, Madrid, Spain). Ddx5 and proliferating cell nuclear antigen were from Abcam. Ddx3x was from Millipore. FLAG clone M2, Vinculin, and Nucleolin were from Sigma-Aldrich, Novus Biologicals, and Novus Biologicals, respectively.

shRNAs. Sequence-verified MISSION shRNA lentiviral plasmids (Sigma-Aldrich) were used to down-regulate *Ddx3x* (TRCN0000103750 and TRCN0000103751), *Ddx5* (TRCN000071103 and TRCN000071104), and *Pbx1* (TRCN0000012575-#1 and TRCN0000012577-#2). shRNA targeting *PREP1* has already been described (1).

Plasmids and Retroviral Infection. pMSCV-puro-*Meis1a* was obtained by cloning FLAG-tagged *Meis1a* cDNA into BglII/XhoI restriction sites of pMSCV-puro retroviral vector. Prep1 deletion mutants have been described (2). The mutants were amplified from the original vectors and subcloned into the XhoI restriction site of pMSCV-hygro vector along with an FLAG-tag. pBabe-hygro-Ras^{v12}, pBabe-puro-*Myc*, and corresponding empty vectors were used. For retroviral transduction of mouse embryonic fibroblasts (MEFs) and IMR32, Phoenix-Eco and Phoenix-Ampho cell lines were used, respectively.

Cell Growth Assay. Indicated numbers of cells were seeded into six-well culture plates in triplicate, and the medium was replaced every day. Depending on the experiment, at the indicated time points, cells were either counted directly with a FastRead 102 disposable counting chamber (Immune Systems) or fixed and stained with crystal violet; the absorbance of the cells was read at 595 nm.

Apoptosis Assay. The number of apoptotic cells was determined using propidium iodide staining and flow cytometry as described (3). Briefly, 1×10^6 cells were fixed in 70% (vol/vol) cold ethanol and suspended in 1 mL staining solution containing 50 μg/mL propidium iodide (Sigma-Aldrich) and 250 μg/mL RNase (Invitrogen) for 3 h at room temperature. Stained cells were analyzed by FACSCalibur (BD Bioscience). Cells having a level of DNA below that level of G1 phase were considered apoptotic.

Gene Expression Analysis. RNeasy mini kit (QIAGEN) was used to perform all RNA extractions, and genomic DNA was degraded with RNase-free DNaseI (New England Biolabs); 1 μg total RNA was retrotranscribed in buffer containing dNTPs, RNase OUT, random primers, and superscript III reverse transcriptase (Invitrogen). Semiquantitative PCR was carried out on the GeneAmp PCR system a700 (Life Technologies) using the following primers: forward primer, 5′-ATGATGGCTACACAGACATTAAG-3′ and reverse primer, 5′- CTACTGCAGGGAGTCACTGTTC-3′. For Prep1Δ carboxy terminal domain, the following reverse primer was used: 5′-TTACATTGGCTGAAGAATTGGTC-3′.

Quantitative real-time PCR was performed using SYBR Green PCR Master Mix on a Roche Light Cycler 480 using specific *Meis1* primers (4). *GAPDH* was used as control to normalize the results (1). For all experiments, reverse transcriptase minus controls was performed.

Pull-Down Assay. *Meis1a* and *Pbx1b* fragments were amplified from the cDNA pool prepared from MEFs using the following primers.

Meis1a: Forward, 5′-ATGGCGCAAAGGTACGACGAC-3′; reverse, 5′-TTACATGTAGTGCCACTGCC-3′.

Pbx1b: Forward, 5′- ATGGACGAGCAGCCGAGGC-3′; reverse, 5′- TCACTGTATCCTCCTGTCTGGCTG-3′.

The amplified fragments were digested by EcoRI-XhoI (*Meis1a*) or BamHI-XhoI (*Pbx1b*) double digestions and cloned in frame with the GST of pGEX-6p-1 vector (GE Healthcare). All constructs were verified by sequencing them in both directions. GST-Prep1 and GST-fusion proteins production and purification have been described (5). Meis1a and Prep1 were cleaved from GST by PreScission protease. For pull-down assays, 60 μg GST-Pbx1b was bound to 40 μL 50% glutathion-sepharose 4B bead as previously described (5). Indicated amounts of purified Meis1a and Prep1 were mixed with GST-Pbx1b, which adsorbed to glutathion-sepharose beads. The binding reaction was carried out for 1 h at 4 °C in 1 mL buffer of 10 mM Tris·HCl (pH 8), 0.2% Nonidet P-40, and 150 mM NaCl. After thoroughly washing with the buffer, 20 μL 2× Laemli sample buffer was added to each sample, boiled for 5 min, and subjected to 10% (vol/vol) SDS-PAGE followed by Western blotting analysis.

Tandem Affinity Purification and MS Analysis. To construct the *Meis1a–tandem affinity purification* (*TAP*) vector, the seamless gene fusion technique by overlap PCR was used (6). TAP cassette was amplified from the pBabe–*Prep1-TAP* vector (7), and the *Meis1a* fragment was amplified from the cDNA pool from MEFs. *Meis1a-TAP* fusion fragments were cloned into XhoI/HpaI sites of pMSCV-puro retroviral vector. The following primers were used for cloning.

Meis1a forward primer: 5′-ATGGCGCAAAGGTACGACGAC-3′.

Meis1a reverse primer + TAP overlap sequence: 5′-*CTTCTCTTTTCCAT*TTGCATGTAGTGCCACTGC-3′.

TAP cassette forward primer: 5′-ATGGAAAAGAGAAGATGGAAAAAGAATTTC-3′.

TAP cassette reverse primer: 5′-TCAGGTTGACTTCCCCGCG-3′.

TAP protocol was performed as previously described (7). The TAP eluates were resolved on 10% (vol/vol) SDS-PAGE. The gel was fixed in 50% (vol/vol) methanol + 10% (vol/vol) acetic acid and stained overnight with the Colloidal Blue staining kit (LC6025; Invitrogen). Different regions were cut out from the gel and trypsinized as previously described (8). Peptides were desalted (9), dried in a Speed-Vac, and resuspended in 7 μL 0.1% TFA. Liquid chromatography–electrospray ionization-MS/MS of 5 μL each sample was performed on a Fourier-transformed LTQ mass spectrometer (Thermo Electron). Peptides separation was performed on a linear gradient from 100% solvent A [5% (vol/vol) acetonitrile, 0.1% formic acid] to 20% solvent B [99.9% (vol/vol) acetonitrile, 0.1% formic acid] over 20 min and from 20% to 80% solvent B in 5 min at a constant flow rate of 0.3 μL/min on an Agilent chromatographic separation system 1100 (Agilent Technologies). The liquid chromatography system was connected to a 10.5-cm fused silica emitter of 100-μm inner diameter (New Objective, Inc.) and packed in-house with ReproSil-Pur C18-AQ 3-μm beads (Dr. Maisch Gmbh) using a high-pressure bomb loader (Proxeon). Proteins were identified by searching a comprehensive

nonredundant protein database (National Center for Biotechnology Information nr) using MASCOT. Nonspecific contaminants (i.e., keratins) were identified after comparison with empty vector-infected (pMSCV-TAP virus) cells and disregarded.

1. Iotti G, et al. (2011) Homeodomain transcription factor and tumor suppressor Prep1 is required to maintain genomic stability. *Proc Natl Acad Sci USA* 108(29):E314–E322.
2. Berthelsen J, Zappavigna V, Ferretti E, Mavilio F, Blasi F (1998) The novel homeoprotein Prep1 modulates Pbx-Hox protein cooperativity. *EMBO J* 17(5):1434–1445.
3. Riccardi C, Nicoletti I (2006) Analysis of apoptosis by propidium iodide staining and flow cytometry. *Nat Protoc* 1(3):1458–1461.
4. Kocabas F, et al. (2012) Meis1 regulates the metabolic phenotype and oxidant defense of hematopoietic stem cells. *Blood* 120(25):4963–4972.
5. Díaz VM, et al. (2007) p160 Myb-binding protein interacts with Prep1 and inhibits its transcriptional activity. *Mol Cell Biol* 27(22):7981–7990.
6. Lu Q (2005) Seamless cloning and gene fusion. *Trends Biotechnol* 23(4):199–207.
7. Díaz VM, Bachi A, Blasi F (2007) Purification of the Prep1 interactome identifies novel pathways regulated by Prep1. *Proteomics* 7(15):2617–2623.
8. Shevchenko A, Wilm M, Vorm O, Mann M (1996) Mass spectrometric sequencing of proteins silver-stained polyacrylamide gels. *Anal Chem* 68(5):850–858.
9. Rappsilber J, Ishihama Y, Mann M (2003) Stop and go extraction tips for matrix-assisted laser desorption/ionization, nanoelectrospray, and LC/MS sample pretreatment in proteomics. *Anal Chem* 75(3):663–670.

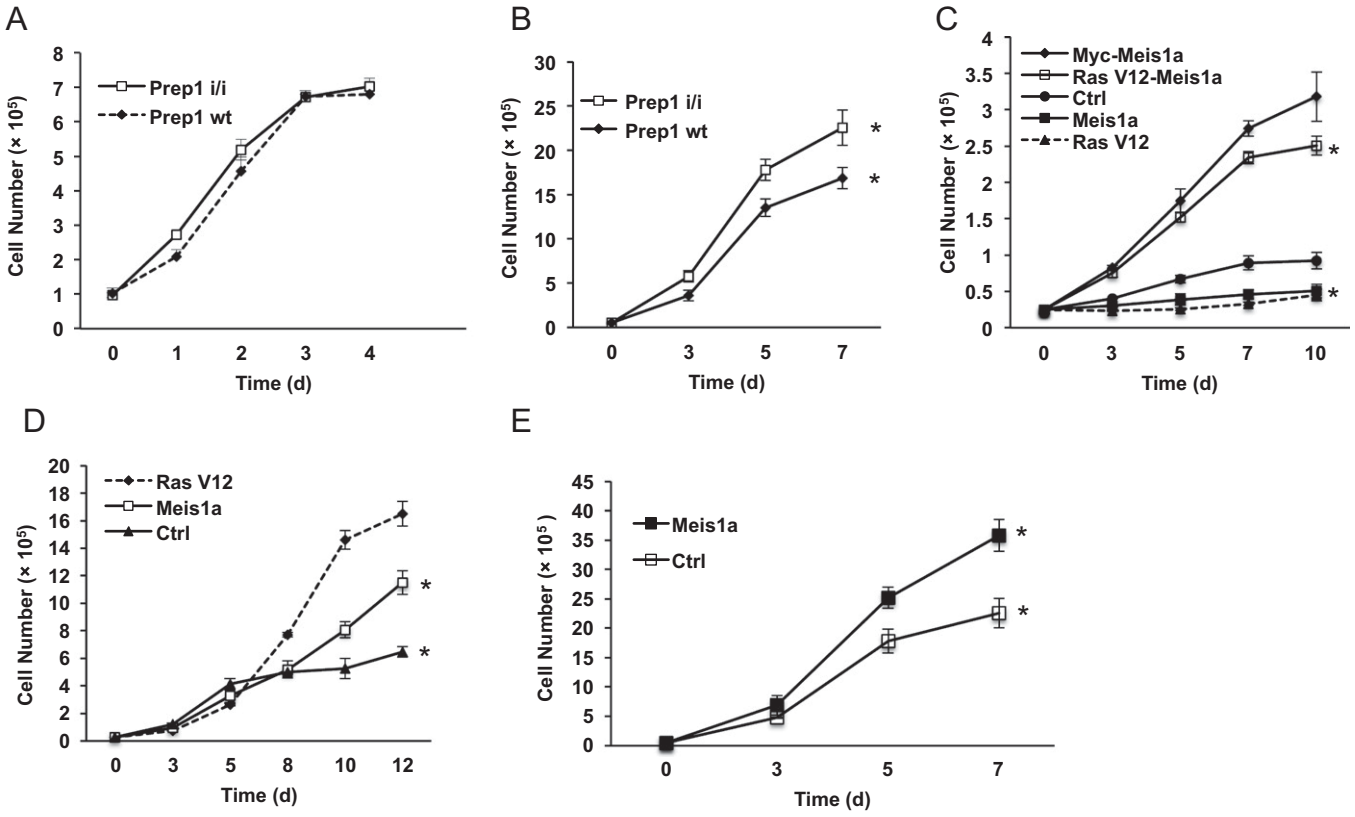

Fig. S1. Proliferation rate of primary and immortalized MEFs. (*A*) WT and *Prep1*$^{i/i}$ primary MEFs grow equally well, but (*B*) immortalized *Prep1*$^{i/i}$ cells grow faster than WT; (*A*) 1×10^5 passage-2 and (*B*) 5×10^4 passage-35 *Prep1*$^{i/i}$ and WT cells were plated in six-well plates in triplicate and directly counted at the indicated time points. Error bars show SD (*$P < 0.05$). (*C*) Meis1a does not induce growth in primary *p53*$^{+/+}$ cells but (*D*) does so in *p53*$^{-/-}$ MEFs; (*C*) 2.5×10^4 passage-3 *p53*$^{+/+}$ or (*D*) *p53*$^{-/-}$ cells infected with the indicated retroviruses were plated in 12-well plates in triplicate and directly counted at the indicated time points. Error bars show SD (*$P < 0.05$). (*E*) Meis1a induces growth in *Prep1*$^{i/i}$ MEFs; 5×10^4 passage-35 *Prep1*$^{i/i}$ cells overexpressing Meis1a were plated in six-well plates in triplicate and directly counted at the indicated time points. Cells infected with empty vector were used as control (Ctrl). Error bars show SD (*$P < 0.05$). The proliferation assay details are given in *SI Materials and Methods*.

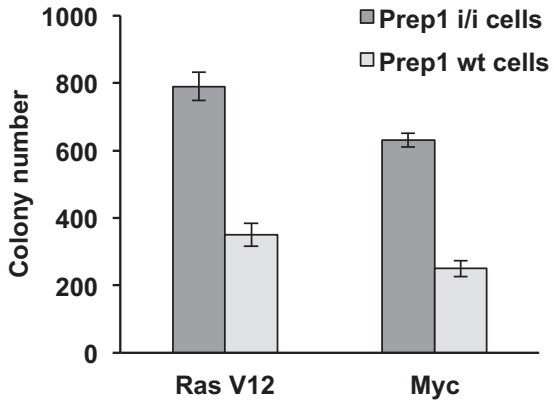

Fig. S2. Ras^{v12} and Myc transformations are more efficient in *Prep1*-deficient than WT cells. The number of colonies generated in soft agar by 1×10^5 cells overexpressing Ras^{v12} or Myc is shown. The experiment was performed in triplicate, and colonies were scored after 10 d.

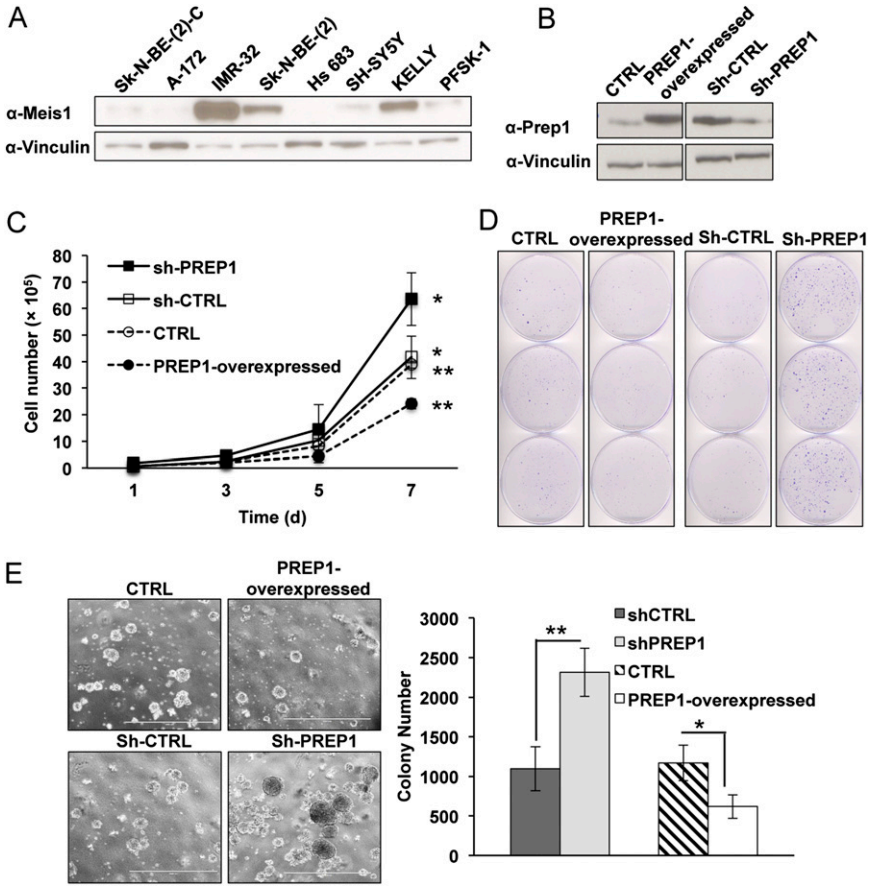

Fig. S3. Effect of PREP1 modulation on proliferation and tumorigenic potential of IMR32 cells. (*A*) IMR32 human neuroblastoma cells express the highest level of Meis1. Eight different human brain tumor cell lines were screened for *MEIS1* expression by immunoblotting. (*B*) Construction of PREP1-overexpressing or PREP1 down-regulated IMR32 cells. Immunoblots show the levels attained in the modified IMR32 cells. (*C*) PREP1 expression affects IMR32 growth rate. Proliferation rate of 1.2×10^5 *PREP1*-overexpressed and knockdown cells plated in 12-well plates is shown at different time points. The experiment was performed in triplicate. Error bars indicate SD (*$P < 0.05$; **$P < 0.01$). (*D*) Down-regulation of PREP1 decreases the colonogenic activity of IMR32 cells. Colony assays show the effect of PREP1 modulation in IMR32 cells; 10 d after plating, cells were fixed and stained. (*E*) PREP1 expression level affects the number and the size of soft agar colonies. Photographs show soft agar growth of *PREP1*-overexpressed or knocked down cells. The number of colonies formed 10 d after plating is shown in *Right*. Error bars indicate SD (*$P < 0.05$; **$P < 0.01$).

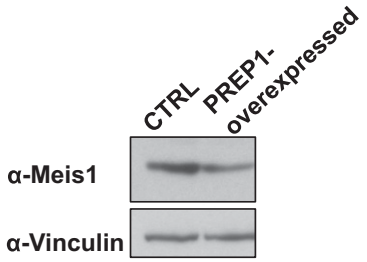

Fig. S4. PREP1 overexpression decreases MEIS1A level in IMR32 cells. Immunoblots show MEIS1A protein level in CTRL and *PREP1*-overexpressed IMR32 cells. Vinculin was used as loading control.

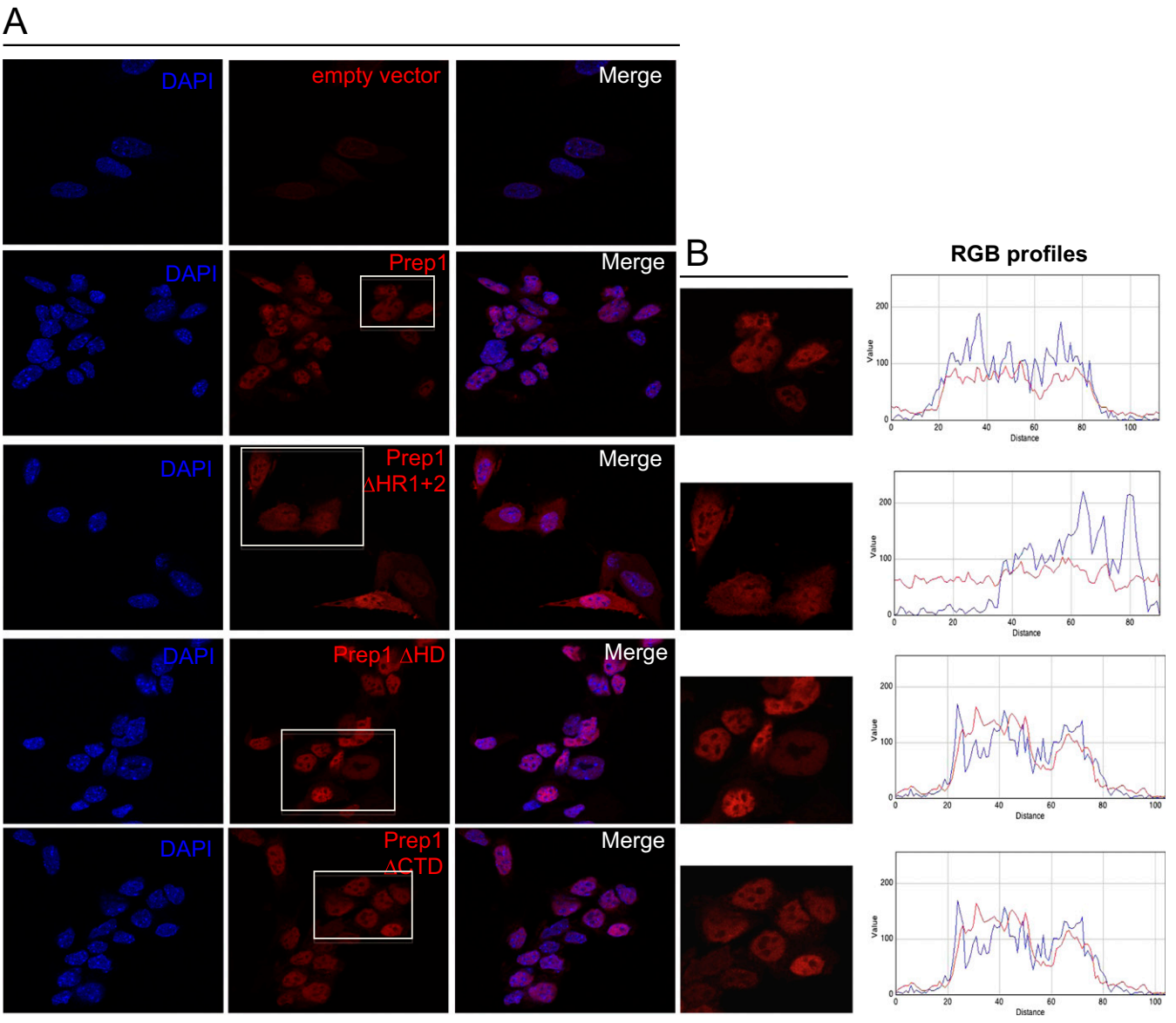

Fig. S5. Subcellular localization of different Prep1 mutants. (*A*) Cells overexpressing different *Prep1* full length and mutants were analyzed by immunofluorescence and confocal microscopy after fixation and staining with DAPI (blue) and Prep1-Cy5 antibody (red). Cells infected with empty vector were used as controls. The nuclear dye DAPI was used to counterstain nuclei. *B* represents the zoom of selected areas shown in *A*. The red, green, blue (RGB) profiles on the right show the extent of colocalization of DAPI (blue line) and Prep1 (red line) staining.

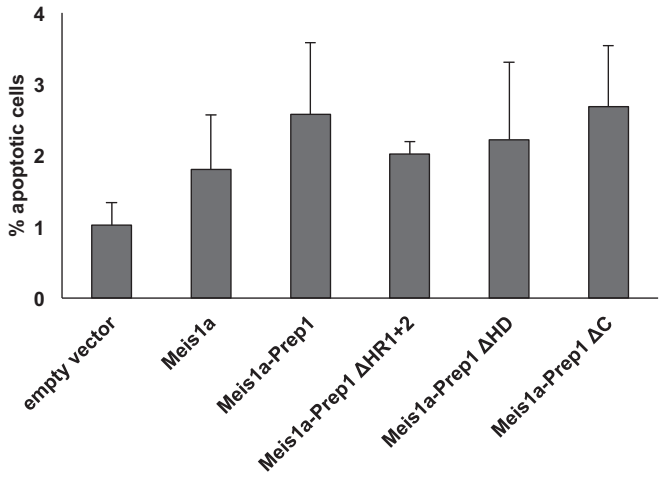

Fig. S6. Effect of Meis1a and different Prep1 mutants on basal apoptotic rate of *Prep1*$^{i/i}$ cells. The number of apoptotic cells was determined by flow cytometry using propidium iodide staining. The graph summarizes the results of two independent experiments. Error bars indicate SD.

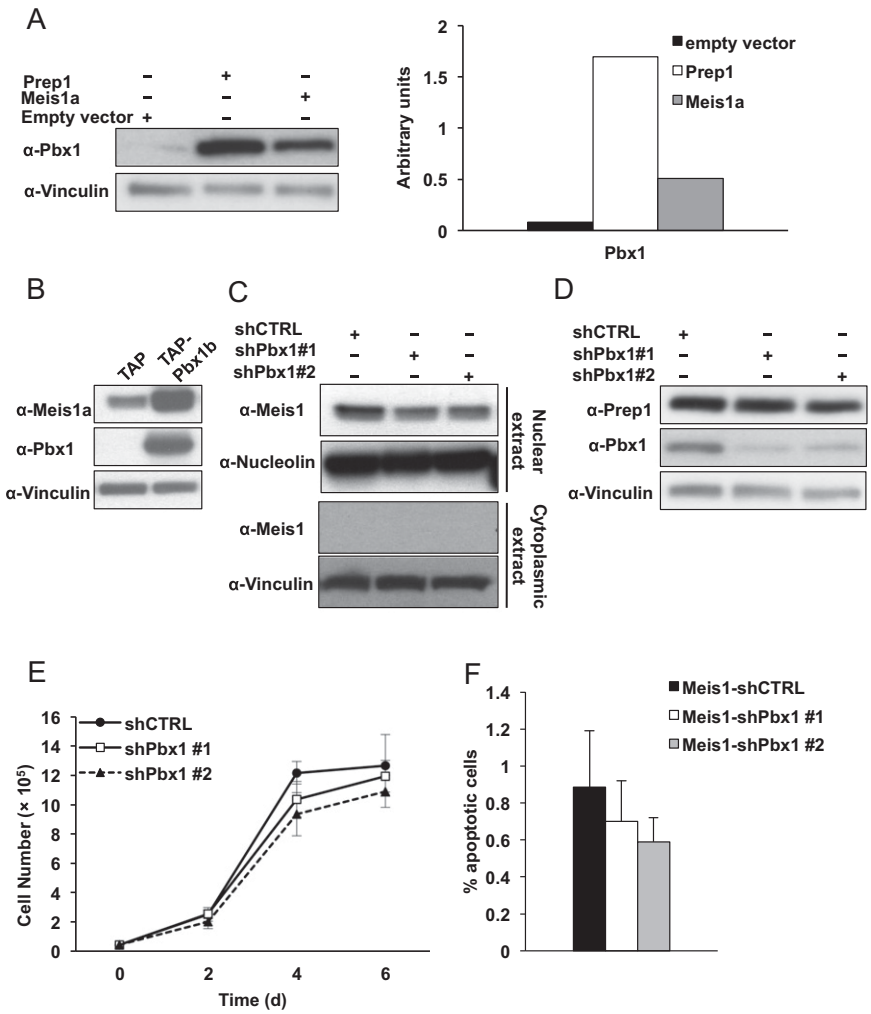

Fig. S7. Although Pbx1 and Meis1a are more stable in complex, *Pbx1* depletion does not affect the growth rate of cells. (*A*) Overexpression of Prep1 or Meis1a increases Pbx1 level. Immunoblots show effect of Prep1 or Meis1a overexpression on Pbx1 protein level. The bar graph in *Right* shows the densitometric quantitation. (*B*) Pbx1b overexpression affects Meis1a expression level. TAP-Pbx1b was overexpressed in *Prep1*$^{i/i}$ cells overexpressing Meis1a. Cells infected with TAP vector were used as controls. Immunoblots show Meis1a and exogenous Pbx1b expression. (*C*) Nuclear and cytoplasmic extracts were analyzed by immunoblotting with anti-Meis1 antibody. Nucleolin and Vinculin were used as loading controls for nuclear and cytoplasmic extracts, respectively. (*D*) Prep1 and Pbx1 levels in shCTRL- and shPbx1-treated cells were checked using anti-Prep1– and anti-Pbx1–specific antibodies. (*E*) Down-regulation of Pbx1 does not affect the growth rate of *Prep1*$^{i/i}$ cells; 5×10^4 *Pbx1*^{kd} *-Prep1*$^{i/i}$ cells overexpressing Meis1a were plated in six-well plates in triplicate and counted at the indicated time points. (*F*) Pbx1 depletion does not affect the basal apoptotic rate of the Meis1a-overexpressing *Prep1*$^{i/i}$ MEFs. The number of apoptotic cells was analyzed by propidium iodide staining and flow cytometry. The graph summarizes the results of two independent experiments. Error bars indicate SD.

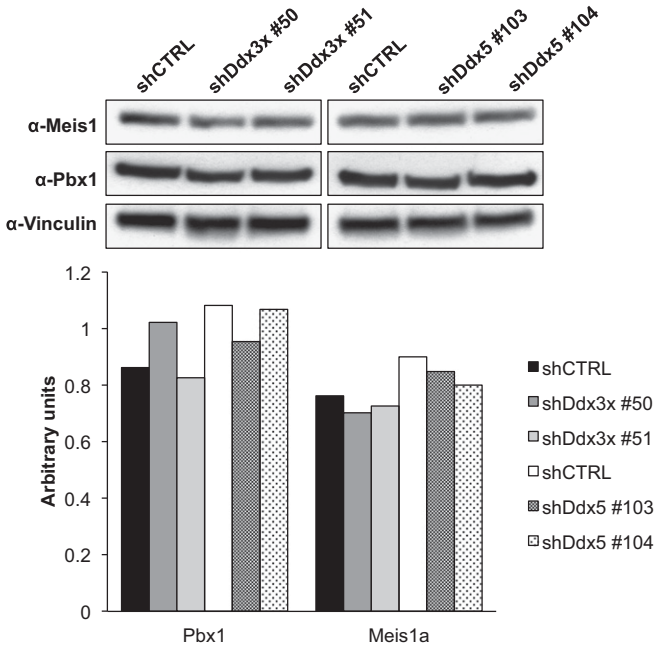

Fig. S8. Ddx3x or Ddx5 down-regulation does not affect Meis1a and Pbx1 protein levels. Immunoblots show Meis1a and Pbx1 protein levels in total cell lysates of shCTRL-, shDdx3x- or shDdx5-treated Meis1a-transduced *Prep1*$^{i/i}$ MEFs. Vinculin was used as loading control.